The Egyptian Journal of Remote Sensing and Space Sciences xxx (2017) xxx–xxx

HOSTED BY

ELSEVIER

Contents lists available at ScienceDirect

The Egyptian Journal of Remote Sensing and Space Sciences

journal homepage: www.sciencedirect.com

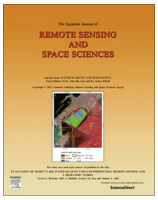

Research Paper

On the classifications of the solar active regions (ARs); Case study for solar cycles 23 and 24

Wael Mohamed [a,*], Shahinaz Yousef [b], Mosalam Shaltout [c]

[a] National Authority for Remote Sensing and Space Sciences, Cairo, Egypt
[b] Astronomy, Space and Meteorology Dep., Faculty of Science, Cairo University, Egypt
[c] National Research Institute of Astronomy and Geophysics, Helwan, Egypt

ARTICLE INFO

Article history:
Received 23 November 2016
Revised 26 March 2017
Accepted 14 April 2017
Available online xxxx

Keywords:
Solar cycle
Declining phase
X-class flare
Active region

ABSTRACT

The declining phase of solar cycle 23 is an important case of study. Many high energetic solar flares occurred in 2003. The occurrence of high energetic solar X-ray flares (X-type) is related to solar cycle's phases and the state of the active regions producing them. In some cases, the declining phases may be more active than the maximum phase. A statistical study is performed for solar flares (X-class) occurrence at declining and maximum phases of solar activity. The relationships between the X-class flares, SSN and active regions (ARs) will be investigated. The active region productivity of X-flares is in coherence with the number of days of ($\beta - \gamma - \delta$) magnetic field. The active regions energies are consumed in the acceleration of protons and production of X-flares among other things (e.g. CME lifting up). The higher the energy of X-flares the lower the proton flux (pfu @ >10 MeV) and vice versa.

1. Introduction

Dodson and Hedeman (1975) explained the three pulses in activity occurred from 1972 to 1974 during the declining part of solar cycle 20. On February 1972, the site of beta spots (latitude N 10° longitude 21°) had 32 flares and sub-flares and were associated with sudden ionospheric disturbances (SID) which was the largest number of SID's occurred with any center of activity during 1972. The increase of activity in N 10° longitude 21° and N 13° longitude 13° lasted approximately from February 1972 through 1973.

Shaltout (1995) commented on the high energetic solar flares that occurred during the year 1991 and have been produced by the active region 6659 (defined by National Oceanic and Atmospheric Administration, NOAA and United States Air Force, USAF). This year is a part of the declining phase of solar cycle 22.

Dyer (2002) described the years around solar maximum (Ascending and Declining phases) of the sun's activity as there is an additional random source of lower energy particles accelerated during certain solar flares and in the subsequent coronal mass ejections (CMEs). These solar particle events lasted for several days at a time and contained both protons and heavier ions with variable composition from event to event. Energies typically range up to several hundred MeV and have most influence on high inclination or high altitude systems. Occasional events produce particles of several GeV in energy and these can reach equatorial latitudes.

The length of declining phase varies from solar cycle to another depending on the amount of energy in the sun not mainly on the maximum sunspot number of the cycle. Solar cycle number 23 is a weak cycle (Yousef, 1995, 2003); it thus had the longest declining phase (5 years) although the maximum sunspot number was 119.6.

In the descending phases, it is found that the sun experiences an activity state in this phase comparable to the maximum phase. In some cases, the declining phases may be more active than the maximum phase. In a way of classifying the solar active regions according the productivity of energetic flare, it is important to study all active regions characteristics of selected solar flares before and at the time of occurrence of the flare.

2. Data and analysis

2.1. Most powerful solar flares ever recorded from 1976 to 2006

The most powerful X-ray flares ever recorded for the period 1976–2006 are compiled by IPS Radio & Space Services (www.spaceweather.com) and reproduced, after determining the phase of solar activity for each flare, in Table 1.

Peer review under responsibility of National Authority for Remote Sensing and Space Sciences.

* Corresponding author.
E-mail address: wael.mohamed@narss.sci.eg (W. Mohamed).

http://dx.doi.org/10.1016/j.ejrs.2017.04.004
1110-9823/

In the third column of Table 1: M means maximum phases, D means declining phases and A means ascending phases.

During the time period from July 11th, 1978 to December 5th, 2006, 30 solar X-class flares have been (from X28 to X9) recorded; 6 flares at maximum (20.0%), 2 flares at ascending phases (6.67%) and 22 flares at the declining phases of solar cycles (73.33%). Thus, it is greatly probable to observe high energetic solar (X-class) flares at the declining phases of solar cycles.

On the study of the most powerful solar flares, relation between solar proton flux and the X-flares is a point of interest. The sun energy is divided between the X-flare and the proton fluxes of the event. This relation is shown in Table 2 and Fig. 1.

The curve in Fig. 1 can be divided into two sections;

a. Sharp rise, for proton flux <353 pfu. There is a linear relation between X-class flares energy and the proton flux (pfu @ >10Mev).
b. Exponential decay, for proton flux >353 pfu. The increase of solar proton flux (pfu @ >10Mev) is accompanied by a drop in the X-flare energy.

We can explain this in the following manner:

The available energy produced in the active region is divided between the acceleration of protons and the production of X-flares among other things (e.g. CME lifting up). The higher the energy of X-flares the lower the proton flux (pfu @ >10 MeV) and vice versa.

2.2. Solar active regions

Several solar active regions have been studied in order to investigate different active regions capacities of energetic X-flares production.

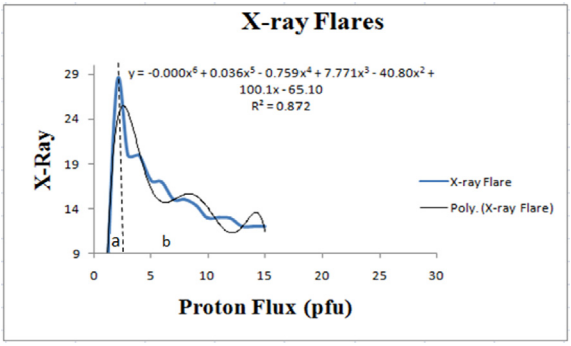

Fig. 1. Relation between solar proton flux and the X-class flares. The dashed line divides the sections of the sharp rise (a) and the exponential decay (b) at energy 353 pfu (@ >10 MeV).

This study involves 30 solar active regions, which produced highly energetic X-flares, as they cross the solar disk. For each region, start and end dates, sunspots numbers, sizes of sunspots, class of magnetic fields, sunspots classification, location and the most powerful 10 solar flares produced from that region. All data set for solar active regions are obtained, from URL: http://www.spaceweatherlive.com/en/solar-activity/region/regionnumber.

2.2.1. Number of days of ($\beta - \gamma - \delta$) configuration and the Corresponding number of X-flares for ARs under study

Beta-Gamma-Delta ($\beta - \gamma - \delta$) magnetic field is considered the strongest of all magnetic field types of sunspots. In this type, a sunspot group has a beta-gamma magnetic configuration however; it also contains one (or more) delta sunspots. A delta type has umbrae of opposite polarities within a single penumbra.

Table 1
The phases of solar cycle for the most powerful solar flare.

Date (d/m/y)	X- Class	Phase of solar activity	Date (d/m/y)	X- Class	Phase of solar activity
4/11/2003	X28+	D	11/6/1991	X12	D
2/4/2001	X20.0	D	15/06/91	X12	D
16/08/89	X20.0	M	17/12/82	X10.1	D
28/10/03	X17.2	D	20/05/84	X10.1	D
7/9/2005	X17	D	29/10/03	X10	D
6/3/1989	X15	M	25/01/91	X10	D
11/7/1978	X15	A	9/6/1991	X10	D
15/04/01	X14.4	D	9/7/1982	X9.8	D
24/04/84	X13	D	29/09/89	X9.8	M
19/10/89	X13	M	22/03/91	X9.4	D
15/12/82	X12.9	D	6/11/1997	X9.4	A
6/6/1982	X12	D	24/05/90	X9.3	M
1/6/1991	X12	D	5/12/2006	X9	D
4/6/1991	X12	D	6/11/1980	X9	M
6/6/1991	X12	D	2/11/1992	X9	D

Table 2
X-ray flares of type X and the proton flux (Pfu @ >10 MeV).

Date (d/m/y)	X-ray Flare	Proton flux unit (pfu @ >10 MeV)	Date (d/m/y)	X-ray Flare	Proton flux unit (pfu @ >10 MeV)
4/11/2003	28+	353	6/6/1991	12	3000
2/4/2001	20	1110	11/6/1991	12	1400
16/08/89	20	9200	15/06/91	12	1400
28/10/03	17.2	29500	17/12/82	10.1	130
7/9/2005	17	1880	20/05/84	10.1	2500
6/3/1989	15	110	29/10/03	10	29500
11/7/1978	15	38	25/01/91	10	240
15/04/01	14.4	951	9/6/1991	10	1400
24/04/84	13	2500	9/7/1982	9.8	2900
19/10/89	13	40000	29/09/89	9.8	4500
15/12/82	12.9	130	22/03/91	9.4	43000
6/6/1982	12	30	6/11/1997	9.4	490
1/6/1991	12	3000	24/05/90	9.3	180
4/6/1991	12	3000	5/12/2006	9	1980

Please cite this article in press as: Mohamed, W., et al.. Egypt. J. Remote Sensing Space Sci. (2017), http://dx.doi.org/10.1016/j.ejrs.2017.04.004

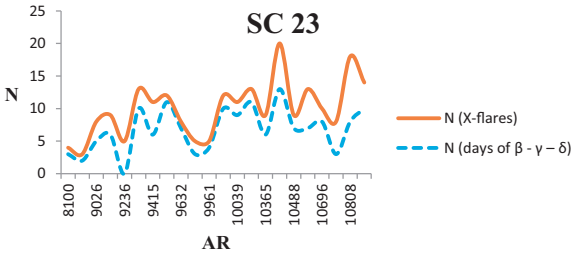

Fig. 2. The relation between (N X-flares) and (N days of β – γ – δ) for AR of solar cycle 23.

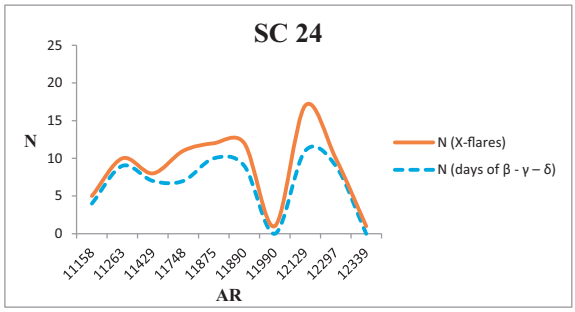

Fig. 3. The relation between (N X-flares) and (N days of β – γ – δ) for ARs of solar cycle 24.

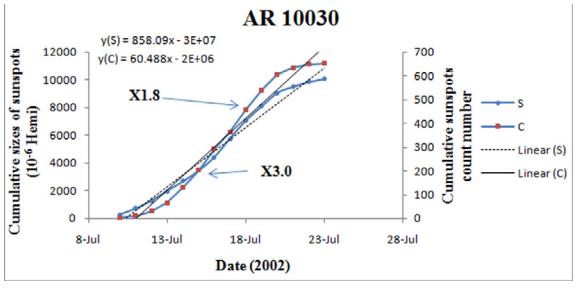

Fig. 4. Cumulation of S and C parameters for high energetic flares for AR 10030.

Table 3
The highest, average and the lowest slopes of S and C parameters of 32 ARs.

Slope	S		C	
	AR	Slope	AR	Slope
Highest	12129	2258.8	**10039**	**758.41**
	10486	2077.2	**9591**	**474.47**
Average	11429	783.3	10030	60.488
Lowest	**10039**	**49.973**	10930	11.654
	9591	**23.293**	11990	5.8143

*Bolded ARs possess both the highest and the lowest slopes of C and S respectively.

By analyzing the number of X-flares and the number of days of (β – γ – δ) magnetic field for solar cycles 23 and 24, It is evident that there is coherence between number of X-flares and the number of days of (β – γ – δ) magnetic field as shown in Figs. 2 and 3 for two cycles 23 and 24 respectively.

For each region, there is a graph was drawn for the relation between sunspots number and the size of this spot at the same day, where S and C parameters are defined for the cumulative summation for the sunspots size and the cumulative summation for the sunspots number, respectively. It also contains the linear fittings for both S and C curves and the equations of fitting.

Table 4
Daily variations of sizes for the 8 ARs under Study.

Day	Size (10^{-6} Hemi)							
	9591	10039	10486	10930	11990	12192	10030	11429
1	60	330	150	390	250	260	280	290
2	280	940	1160	490	180	1240	460	700
3	730	940	1540	430	210	1560	540	770
4	650	850	2200	420	250	2180	690	1120
5	740	940	2170	380	250	2410	730	1270
6	740	900	2180	440	210	2700	780	950
7	620	920	2120	480	190	2740	930	900
8	570	890	2610	680	210	2510	1350	880
9	490	620	2600	670	190	2570	1280	840
10	400	570	2030	620	190	2750	1060	380
11	370	430	1900	550	180	2380	960	410
12	340	480	2160	480	200	2680	460	320
13	260	330	1430	230	110	1500	330	90
14	100		630		60	390	230	
15					60	390		

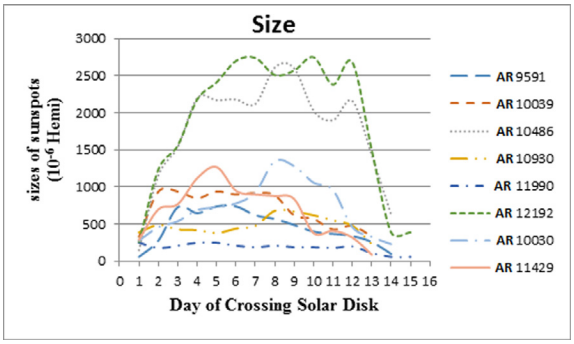

Fig. 5. Daily variations of sizes for the 8 ARs under study.

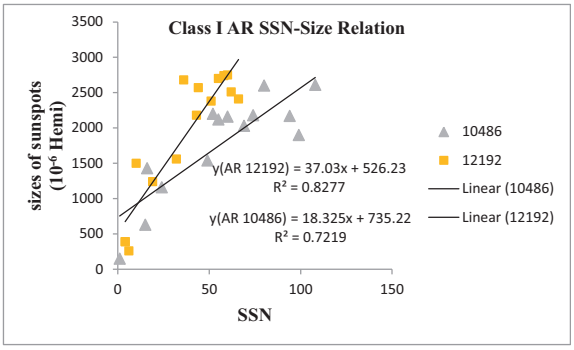

Fig. 6. Relation between AR SSN and size for Class I ARs 10486 and 12192.

For each active region, the cumulative sunspots count number (C parameter) and the cumulative size of sunspots region (S parameter) are calculated for the interval of the active region crossing of the solar visible disk day by day. The curve of S (primary, left, y-axis) and C (secondary, right, y-axis) parameters are plotted versus time (x-axis).All S and C curves have linear general trends. The linear fitting equations are inserted within each active region figure. The R^2 parameter is calculated for each curve to present the degree of fitting. An example for AR number 10030 is shown in Fig. 4 in which the R^2 value is 0.981.

2.2.2. Slope of S and C parameters

From the fitting equations of S and C parameters, the slopes are arranged in descending order. It is a way of selecting active regions as a case study. It is found that the slopes of C for the ARs that

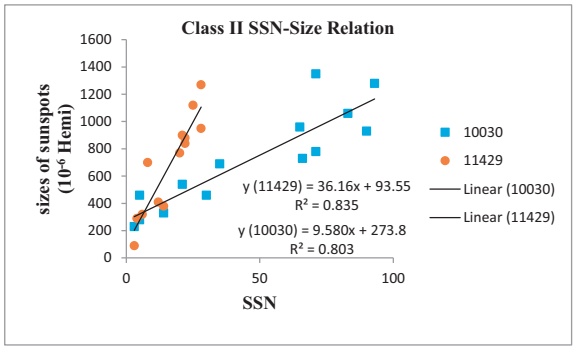

Fig. 7. Relation between SSN and size for Class II ARS 10030 And 11429.

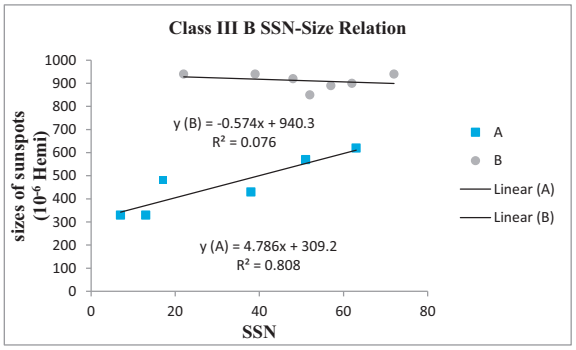

Fig. 9. Relation between SSN and size for Class III B (Composite) AR 10039.

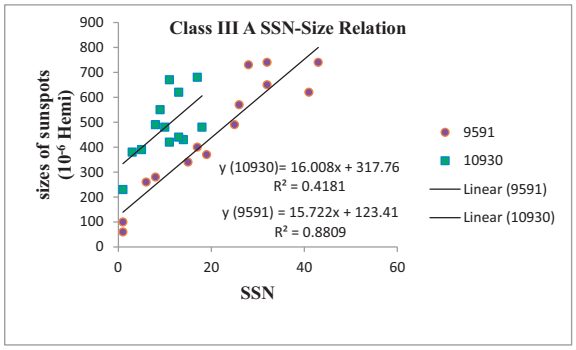

Fig. 8. Relation between SSN and Size for Class III A (Linear) ARs 9591 and 10930.

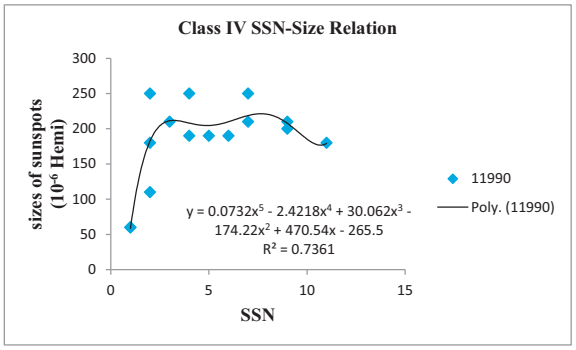

Fig. 10. Class IV (Flat Sizes) for AR 11990.

produced X-class flares vary within the limits ($5.8143 \leq C \leq 758.41$). While the slopes of S for the ARs that produced X-class flares vary within the limits ($23.293 \leq S \leq 2258.8$).

3. Results and discussion

Table 3 shows the ARs with the highest, the average and the lowest slopes for S and C curves.

Table 4 and Fig. 5 present the daily variations of sizes for the 8 ARs under study

In the case of the daily variation of sizes (Fig. 5): There are four distinguished groups of ARs.

Class I: $S \geq 2000 \cdot 10^{-6}$ Hemisphere. Examples are AR 10486 and AR 12192.

Class II: $1000 \leq S \leq 2000 \cdot 10^{-6}$ Hemisphere Examples are AR 10030 and AR 11429.

Class III: $300 \leq S \leq 1000 \cdot 10^{-6}$ Hemisphere Examples are ARs 9591, 10039, and 10930.

Class IV: $S \leq 300 \cdot 10^{-6}$ Hemisphere (Flat sizes). Example is AR 11990.

Further classification according to the sunspot number – size relation will be explained in the following section.

3.1. Relation between ARs sunspot number and sizes

This section concentrates on the ARs SSN – size relation.

Fig. 6 shows the Class I SSN – Size relation.

Fig. 7 shows the Class II SSN– Size relation.

Class III (**$300 \leq S \leq 1000$** 10^{-6} Hemi.) is subdivided into A and B according to the shape of SSN – size relation curve:

Class III A shows a linear relation between the AR SSN and the size as shown in Fig. 8 for AR 9591 and AR 10930.

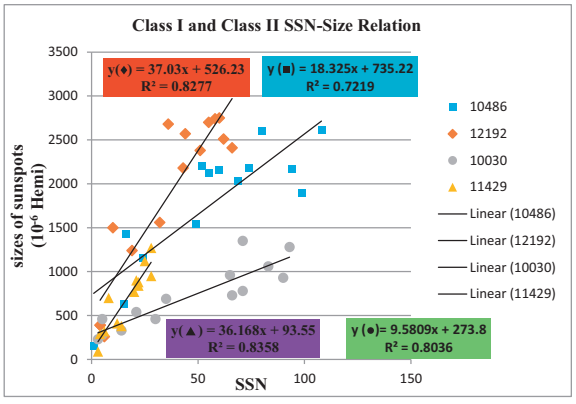

Fig. 11. Comparison between Class I and Class II ARS SSN-Size Relation. Note the difference in size between Class I ($S \geq 2000$ 10^{-6} Hemi.) and Class II ($1000 \leq S \leq 2000$ 10^{-6} Hemi.). The fitting equations and R^2 are presented in the same color for each AR.

Class III B shows composite SSN – size relation for AR 10039 as represented in Fig. 9.

Class IV (flat sizes) is represented by AR 11990 in Fig. 10.

More illustration for the SSN-size relation for Class I and Class II solar ARs is presented in Fig. 11. There is a difference in size between Class I ($S \geq 2000$ 10^{-6} Hemi.) and Class II ($1000 \leq S \leq 2000$ 10^{-6} Hemi.). The fitting equations and R^2 are presented in the same color for each AR.

4. Conclusions

The occurrence of high energetic solar flares (X-class flares) isn't only probable at maximum solar activity, but also there is a great

probability for the occurrence of those flares at other activity phases with special emphasis on the declining phases.

The available energy produced in the active region is divided between the acceleration of protons and the production of X-flares among other things (e.g. CME lifting up). The higher the energy of X-flares the lower the proton flux (pfu @ >10 MeV) and vice versa.

There is coherence between number of X-flares and the number of days of ($\beta - \gamma - \delta$) magnetic field emphasizing the role of magnetic field in the production of X-class flares.

Solar active regions (ARs) of solar cycles 23 and 24 can be classified – according to the daily variation of size – into four classes.

Also, it can be concluded that the production of high energetic X-flares from an AR is a function of all characteristics of the ARs. So, it is necessary to perform a mathematical model for predicting the occurrence of high energetic solar X-flares through the study of solar active regions characteristics such as the sunspot number, the size of the region, the introduced classification of SSN-size relation, the magnetic class of the region and the distribution of the magnetic field lines day by day for all the periods of crossing the region for the solar visible disk.

References

Dodson, H.W., Hedeman, E.R., 1975. Comments on the course of solar activity during the declining phase of solar cycle 20 (1970–74). Solar Phys. 42, 121–130.

Dyer, C., 2002. Radiation effects on spacecraft and aircraft. ESA Publ. Div., 505–512

Shaltout, M.A., 1995. High Energetic Proton Flare on The Declining Phase of Solar Cycle 23. In: Proceedings' of the fourth United Nations/European Space Agency Workshop, held in Cairo, Egypt, Astrophys. and Space Sci., 228:1–2.

Yousef, SH.M., 1995. The downturn of solar activity during the coming three solar cycles. Bull. Fac. Sci., Cairo University, 63: 185.

Yousef, SH.M., 2003. Cycle 23, the First of Weak Solar Cycles Series and the Serious Implications on Some Sun-Earth Connections. In: Proceedings of ISCS, European Space Agency esa.SP-535.Solar Variability as an input to The Earth's Environment, 23–28 June, Tatranska Lomnica, Slovak Republic, 177–180.

Please cite this article in press as: Mohamed, W., et al.. Egypt. J. Remote Sensing Space Sci. (2017), http://dx.doi.org/10.1016/j.ejrs.2017.04.004